

DEVELOPMENT OF A MAGNETICALLY BORNE ELECTRICAL MOTOR PROTOTYPE

Elkin Ferney Rodriguez Velandia

UFF, PGMEC, r. Passo da Pátria 156, Niterói/RJ, 24210-240, Brasil
elkinrodvel@msn.com

José Andrés Santisteban

UFF, PGMEC, TEE, r. Passo da Pátria 156, Niterói/RJ, 24210-240, Brasil
jasantisteban@vm.uff.br

Roberto Firmento de Noronha

UFF, PGMEC, TEM, r. Passo da Pátria 156, Niterói/RJ, 24210-240, Brasil
roberto_noronha@vm.uff.br

Victor Antonio Paiva Silva

UFF, TEE, r. Passo da Pátria 156, Niterói/RJ, 24210-240, Brasil
victorpaivarj@yahoo.com.br

Abstract. *The magnetic bearing is an electro-mechanical device that maintains the rotor of an equipment magnetically levitated. Besides allowing for a contact less working condition, resulting in a system without mechanical wear, this device presents other advantages, such as self-balancing, vibration control, self-monitoring, possibility of equipment encapsulation and high operation speed, with high reliability and reduced maintenance. Taking these advantages into account, magnetic bearings are becoming technologically competitive in many applications such as turbo-generators, pumps, compressors, fabrication machines, gyroscopes, centrifuges etc. It should be realized that since the absence of friction eliminates the need of lubrication, the magnetic bearings are ideal for airspace applications and for radioactive environments. Moreover, due to this same characteristic, it is an energy-saving device, which is, perhaps, the main reason for its utilization in new equipments. In order to gain a better understanding of this technology, a prototype of an integrally levitated electrical motor has been developed. The mechanical, magnetic and electric conceptions of the bearings have been already described in previous works, including the mechanical engineering considerations related to the design, fabrication and mounting of the magnetic bearings on the equipment. In this work, the successfully design and implementation of the displacement controllers are described. Simulations and experimental results show the static and dynamic performance of the bearings.*

Keywords: *magnetic bearings, rotor modeling, closed loop control*

1. Introduction

The development of efficient rotor bearings has been an ever-present concern since the beginning of the Industrial Revolution. The currently employed solutions are the rolling and the journal bearings, which, as a common characteristic, present high energy dissipation due to viscous friction. Innovations in this area lead to the development of the so-called magnetic bearings, which tend to replace the present bearings in some areas of application.

These devices, by means of magnetic forces, are capable to maintain the machine rotor levitating, that is, completely free of any mechanical contact with non-rotating components, drastically reducing the excessive energy losses caused by friction. The efficiency improvement that this technology allows is one of the main reasons for its employment on modern equipment. When compared to traditional ones, the magnetic bearings also present other advantages, such as the capability of self-balancing, vibration control, self-monitoring, possibility of equipment encapsulation and high operation speed, with high reliability and reduced maintenance.

Some examples of successful employment of magnetic bearings are mentioned in literature, such as on high speed gas compressors and other turbo machinery, and also on milling machines (Schweitzer et al, 1994, Kyung and Lee, 2002). Some of these machines may operate on a vertical position, where the radial bearings are not submitted to the rotor weight, while others may operate horizontally, with the radial bearings having to compensate for the rotor weight and for additional lateral loadings due to the function that the machine has to perform, such as milling.

Under this vision, a research line on magnetic bearings is being developed at the Fluminense Federal University. It began with the development of a preliminary prototype, a rotor with only one radial magnetic bearing, whose aim was the appropriation of the basic working principles (Noronha et al, 2000). Presently, a second prototype is under development, whose basic goal is to achieve a development level closer to a finished product. Therefore, for this second prototype, a horizontal, completely levitated rotor was considered, requiring a closed loop control with five degrees of freedom. With this in mind, the electromagnetic design, the control system and, particularly, the mechanical mounting requirements had to be jointly taken into account.

In order to facilitate the transference of this technology to the Brazilian industry, an asynchronous, three phase, two pole and two HP (1500 W) motor was purchased and the modifications that were required in order to introduce a new rotor support system were analyzed. For the same reason, the electronic circuits, needed for the implementation of the current sources that were required to feed the magnetic bearing coils, were designed in such a way that it satisfied not only the requirements of energy economy and reliability, but, above all, that the components were found in the Brazilian market. In short, as it was an interdisciplinary research, the design criteria had to attend not only the electromagnetic requirements of the support system, but also the mechanical considerations relative to the prototype fabrication and assembly.

After the well successful motor adaptation, the following steps were directed toward the implementation of digital displacement controllers. For this, a rigid body model for the rotor was adopted initially. In this model orthogonal displacements are coupled even in zero speed. Nevertheless, displacement controllers were designed and implemented adopting a decentralized control strategy. Experimental results without other radial load than the own rotor weight shows that these controllers were robust. Tests were realized for different speeds, going from zero to 5600 rpm.

2. The prototype construction

In order to have a practical industry application, the guidelines for the electromagnetic design were that the dimensions of the original electric motor should be kept, whenever possible, and the mechanical assembly should be simple and robust. Based on these guidelines, some geometrical parameters were adopted. At each end of the rotor of the electric motor, a radial and an axial bearing were contemplated, which, although physically integrated in one rotor, operate independently.

The analytical design of the magnetic bearings was validated through numerical simulation of the magnetic fields, using the ANSYS Finite Element program (Santisteban et al, 2004). The material specification of radial magnetic bearing was based on the production line of a Brazilian silicon steel sheet producer (Acesita). From the magnetic properties of specified silicon steel and based on an iterative procedure (Chapetta, 2002), the dimensions of the radial bearings were specified, including the number of turns, wire gauge, radius and height of the windings. The same procedure was applied to the axial bearings, except that, in this case, the material was plain carbon steel. The inner and outer edges of the axial bearing stators were specified to have the same section area, in order to equalize the magnetic flux on the axial direction. The design specifications of the radial and axial loads were 200N and 60N, respectively. The complete mass of the modified rotor was found to be 5.304 kg.

The dimensional design of the magnetic bearing covers was based on the dimensions of the motor casing, on the dimensions and position of the radial and axial stators, of the displacement sensors and of the backup rolling bearings, while also taking into account holes for the passage of wires and screws to fix the components into place. All the components present at the covers required great precision on their relative positioning among themselves and in relation to the cover, the motor casing and the rotors. A great deal of effort and attention was required to design and machine the covers and to place the components inside, taking into account the required close tolerances and gaps. The same effort and attention was also required in the machining of the components. All the mechanical components were fabricated at the Machining Laboratory of UFF.

In Fig. 1, left, is shown one radial bearing stator. Their eight coils can generate four resultant magnetic forces that operate in a differential manner, at the horizontal and vertical direction, e.g., to attract the rotor upwards, the resultant force created by the upper coil pair is increased, while the one created by the lower pair is decreased.

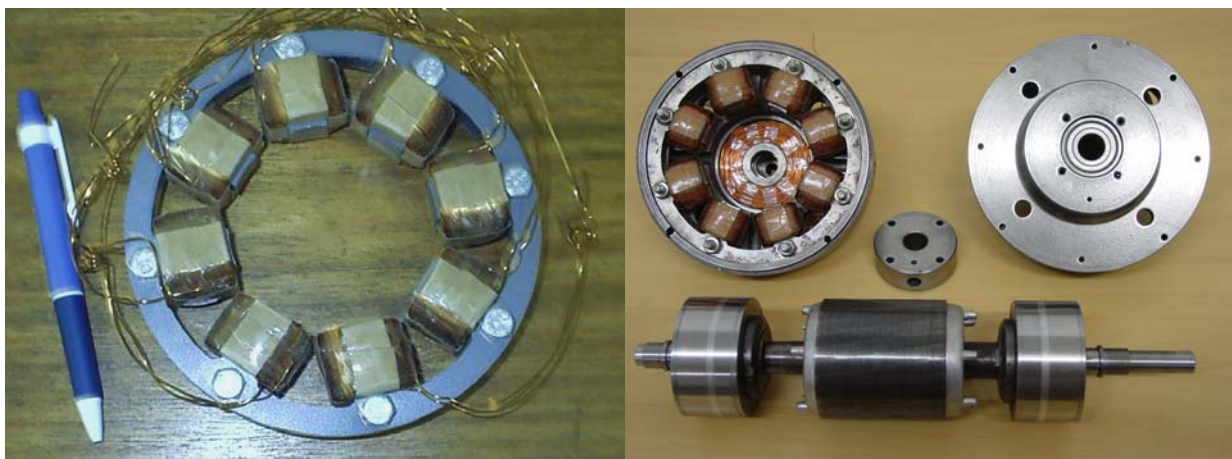


Fig. 1. Magnetic bearing details.

The stators of the axial magnetic bearings are composed of one coil each, producing a magnetic flux path that is closed by the axial airgaps and the axial bearing part of the magnetic bearing rotor. Hence, only one resultant Maxwell force is produced per bearing, which are opposed, one bearing to the other, and also operate in a differential way. Relative to the geometrical axis of the motor, these magnetic flux paths are axisymmetric.

The magnetic fields produced by the radial and axial magnetic bearing stators act upon the same component, the magnetic bearing rotor. As implicitly explained above, there is one axial magnetic bearing rotor placed at each side of the equipment shaft. The plane surfaces, external to the two bearing rotors, receive the axial action, while the cylindrical surfaces receive the radial action. In Fig. 1, right, the whole rotor shaft supporting the motor rotor and the magnetic bearing rotors are shown. In the same figure, upper, can be seen the two covers that in a compact way hold the stators of magnetic bearings. These covers also hold four inductive displacement sensors, axially displaced from the bearing stators, but located on the symmetry planes of the four radial magnetic pole pairs. In order to enhance their response, each pair of radially opposing transducers also works in a differential way. Axial displacements, however, are measured by only one sensor. At the center, the rotation transducer cap is shown.

Finally, for backup purposes, ball bearings were installed on the end covers, to allow the rotor to coastdown if the magnetic bearings fail in operation. The radial gap between these ball bearings and the shaft are smaller than the airgaps between the stators and rotors of the magnetic bearings and of the electrical motor, in order to prevent any contact and any damage to the parts. In Fig. 2 the complete prototype is shown.



Fig. 2. Mounted prototype.



Fig. 3. Current power supplies.

3. The control development

In order to control the winding currents of the magnetic bearings, ten current power supplies were implemented (Santisteban et al 2004). In the electronic structure, signals coming from current sensors are compared with current references. These current references are generated from the position controllers implemented in a personal computer. In Fig. 3 the complete current power supplies module is shown.

Regarding the control system, the controllers for all five degrees of freedom of this system have already been designed and simulated, using a decentralized strategy. Now, based on previous experiences of controlling isolated radial and axial magnetic bearings (Noronha et al, 2000, Santisteban and Mendes, 2003), a control program, written in C, has been implemented. In the following, the radial controller design is described.

According to Schweitzer (1994), the axis was modeled as:

$$\mathbf{f}_B = \mathbf{M}_B \ddot{\mathbf{Z}}_B + \mathbf{G}_B \dot{\mathbf{Z}}_B \quad (1)$$

where \mathbf{f}_B is the column vector representing all the radial magnetic forces and column vector \mathbf{Z}_B represent all the radial measured displacements. \mathbf{M}_B and \mathbf{G}_B are originated from linear algebraic transformations, where:

$$\mathbf{M}_B = \mathbf{T}_B^T \cdot \mathbf{M} \cdot \mathbf{T}_B, \quad \mathbf{G}_B = \mathbf{T}_B^T \cdot \mathbf{G} \cdot \mathbf{T}_B \text{ and:}$$

$$\mathbf{M} = \begin{bmatrix} m & 0 & 0 & 0 \\ 0 & I_y & 0 & 0 \\ 0 & 0 & m & 0 \\ 0 & 0 & 0 & I_x \end{bmatrix}, \quad \mathbf{G} = \begin{bmatrix} 0 & 0 & 0 & 0 \\ 0 & 0 & 0 & 1 \\ 0 & 0 & 0 & 0 \\ 0 & -1 & 0 & 0 \end{bmatrix} I_z \Omega, \quad \mathbf{T}_B = \frac{1}{b-a} \begin{bmatrix} b & -a & 0 & 0 \\ -1 & 1 & 0 & 0 \\ 0 & 0 & b & -a \\ 0 & 0 & -1 & 1 \end{bmatrix}.$$

Above, ‘ m ’ is the net mass of the shaft, that include the rotor of the motor, I_x , I_y and I_z are the inertia moments in respect to the center of mass of the rotor and Ω is the motor rotational velocity. \mathbf{T}_B is used to transform the center of mass coordinates into the magnetic bearings coordinates, one for each axis. Finally, ‘ a ’ and ‘ b ’ are the distances from the rotor center of mass to each radial magnetic bearing.

To design the controllers Eq. (1) can be transformed as in Eq. (2) below, where \mathbf{M}_{Bi} is the inverse of matrix \mathbf{M}_B and $\mathbf{MG} = \mathbf{M}_{Bi} \times \mathbf{G}_B$.

$$\ddot{\mathbf{Z}}_B = \mathbf{M}_{Bi} \times \mathbf{f}_B - \mathbf{MG} \times \dot{\mathbf{Z}}_B \quad (2)$$

The matrix \mathbf{M}_{Bi} and \mathbf{MG} have the following forms:

$$\mathbf{M}_{Bi} = \begin{bmatrix} \frac{(ma^2 + I_y)}{mI_y} & \frac{mab + I_y}{mI_y} & 0 & 0 \\ \frac{mab + I_y}{mI_y} & \frac{mb^2 + I_y}{mI_y} & 0 & 0 \\ 0 & 0 & \frac{(ma^2 + I_x)}{mI_x} & \frac{mab + I_x}{mI_x} \\ 0 & 0 & \frac{mab + I_x}{mI_x} & \frac{mb^2 + I_x}{mI_x} \end{bmatrix}$$

$$\mathbf{MG} = \begin{bmatrix} 0 & 0 & \frac{aI_z\Omega}{I_y(a-b)} & -\frac{aI_z\Omega}{I_y(a-b)} \\ 0 & 0 & \frac{bI_z\Omega}{I_y(a-b)} & -\frac{bI_z\Omega}{I_y(a-b)} \\ -\frac{aI_z\Omega}{I_x(a-b)} & \frac{aI_z\Omega}{I_x(a-b)} & 0 & 0 \\ -\frac{bI_z\Omega}{I_x(a-b)} & \frac{bI_z\Omega}{I_x(a-b)} & 0 & 0 \end{bmatrix}$$

This leads to a block diagram with four inputs and four outputs as shown below:

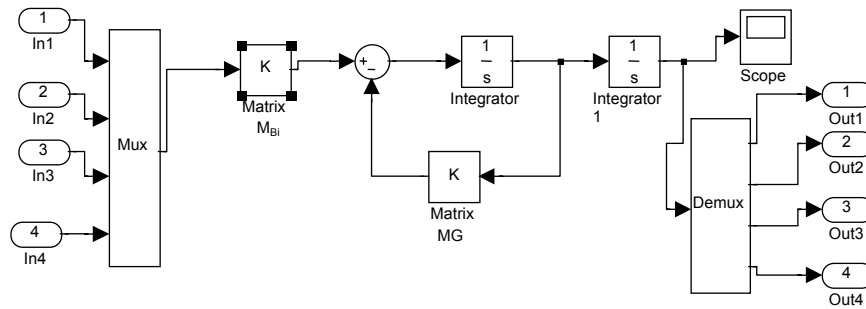


Fig. 4. Mechanical model of the rotor.

The four input forces are generated by the radial magnetic bearings, which, as known, have a non-linear behavior. For example, for an end of the shaft, net forces on axis x and y are given respectively by:

$$f_x = f_4 - f_3 = k \cdot \left(\frac{(i_{bias} + i_{ctrlx})^2}{(h_0 - x)^2} - \frac{(i_{bias} - i_{ctrlx})^2}{(h_0 + x)^2} \right), \quad (3)$$

$$f_y = f_1 - f_2 = k \cdot \left(\frac{(i_{peso} + i_{bias} + i_{ctrly})^2}{(h_0 - y)^2} - \frac{(i_{bias} - i_{ctrly})^2}{(h_0 + y)^2} \right). \quad (4)$$

Where h_0 is the air gap distance at the equilibrium position, x and y are the displacements from equilibrium, i_{bias} is a nominal current reference related to the stiffness, i_{peso} is an additional reference current used for the superior winding on y axis to compensate the weight of the rotor, i_{ctrlx} and i_{ctry} are the control currents coming from the displacement controllers, and k is given by:

$$k = \frac{1}{4} \mu_0 N^2 A \cdot \cos \alpha$$

Where μ_0 is the magnetic permeability of the air, N is the number of turns of the winding, A is the pole cross section, and α is the half opening angle of the pole pair.

After a linearization procedure, from Eq. (3) and Eq. (4), two relationships can be obtained, one for the net force in the horizontal direction and the other for the vertical direction.

$$f_x(i_{ctrlx}, x) = K_{ix} \cdot i_{ctrlx} + K_{sx} \cdot x \quad (5)$$

$$f_y(i_{ctry}, y) = K_{iy} \cdot i_{ctry} + K_{sy} \cdot y \quad (6)$$

Where K_{ix} , K_{iy} , K_{sx} and K_{sy} are constant values obtained from the equilibrium condition.

Joining these relationships with the diagonal terms of matrix \mathbf{M}_{bi} of the mechanical model, and considering null or slow rotor speed, which means that the influence of Matrix \mathbf{MG} is small, and the effect of the non-diagonal terms of \mathbf{M}_{bi} as perturbations, four transfer functions can be obtained, one for each radial direction (Eq. 7 to 10). This result was obtained choosing i_{bias} and i_{peso} in order to obtain the same poles in all the transfer functions. In this way, the design of one common PID controller was possible using the root locus method.

$$G1(s) = K_{ix} \cdot (m \cdot a^2 + I_y) / (I_y \cdot m \cdot s^2 - (m \cdot a^2 + I_y) \cdot K_{sx}) \quad (7)$$

$$G2(s) = K_{ix} \cdot (m \cdot b^2 + I_y) / (I_y \cdot m \cdot s^2 - (m \cdot b^2 + I_y) \cdot K_{sx}) \quad (8)$$

$$G3(s) = K_{iy} \cdot (m \cdot a^2 + I_x) / (I_x \cdot m \cdot s^2 - (m \cdot a^2 + I_x) \cdot K_{sy}) \quad (9)$$

$$G4(s) = K_{iy} \cdot (m \cdot b^2 + I_x) / (I_x \cdot m \cdot s^2 - (m \cdot b^2 + I_x) \cdot K_{sy}) \quad (10)$$

The transfer function of the PID controller is arranged to be given as:

$$G_c(s) = K_c \left[\frac{(s + \beta) \cdot (s + \theta)}{s \cdot (s + \eta)} \right] \quad (11)$$

where K_c is the controller gain and β , θ and η are the controller poles chosen to give stability to the closed loop system. Then, substituting the real parameters in Eqs. (7) to (10), the controller design leads to $\beta = 445 \text{ sec}^{-1}$, $\theta = 10.2 \text{ sec}^{-1}$ and $\eta = 5000 \text{ sec}^{-1}$. Thus, the transfer function of the controller is given by:

$$G_c(s) = K_c \left[\frac{(s + 445) \cdot (s + 10.2)}{s \cdot (s + 5000)} \right] \quad (12)$$

In Fig. 5 are shown the root locus of the four open loop transfer function for each axis. As expected all the root locus diagrams are similar.

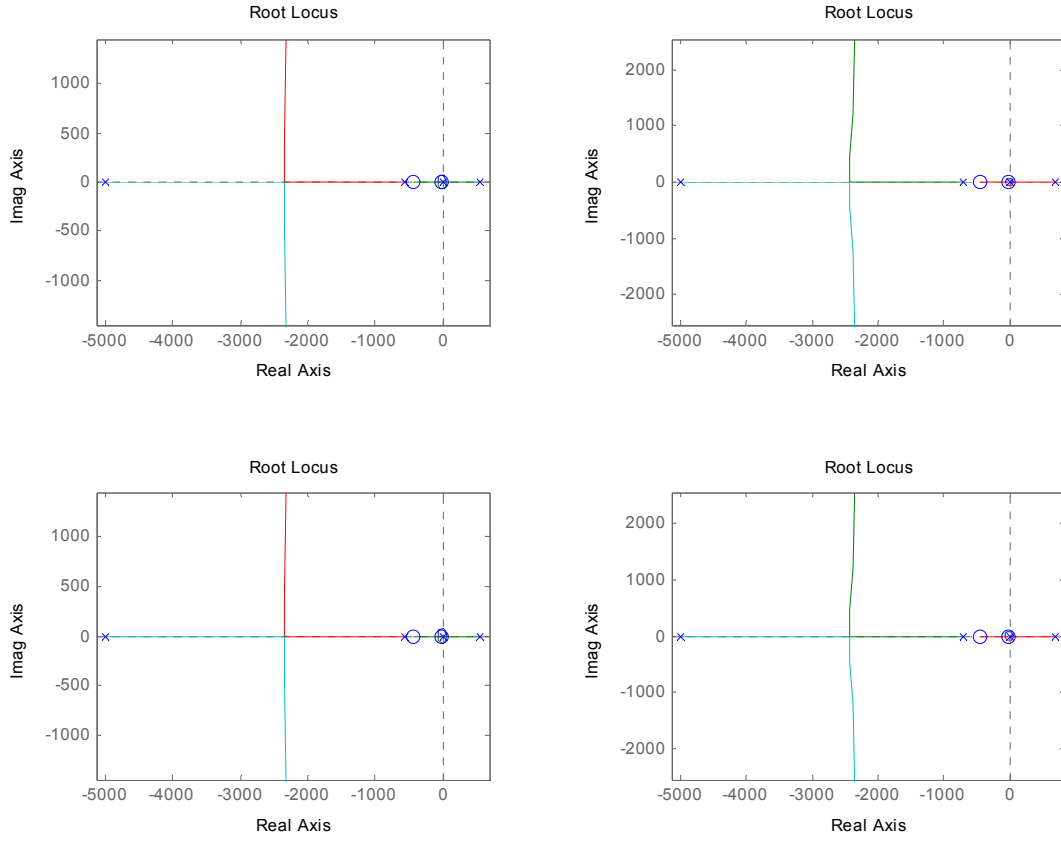


Fig. 5. Root locus for the open transfer function controller and plant.

Finally, with a sampling rate of 1kHz and using the Tustin approximation (Ogata, 1970, 1994), the discrete controller is found to be:

$$G_c(z) = K_c \frac{0.3511z^2 - 0.5708z + 0.221}{z^2 - 0.5714z - 0.4286}. \quad (13)$$

So the difference equation that relates the position error ε and the control current i_{ctrl} is:

$$i_{ctrl(k)} = K_c (0.3511\varepsilon_k - 0.5708\varepsilon_{k-1} + 0.221\varepsilon_{k-2}) + 0.5714i_{ctrl(k-1)} + 0.4286i_{ctrl(k-2)}, \quad (14)$$

where subscript k is related to the sampling time.

4. Experimental Results

A personal computer, an A/D card and a D/A card were used in order to implement the digital controllers. The sampling rate was fixed in 1kHz. One commercial voltage inverter and reduction transformers were employed to furnish AC voltage to the stator windings with variable frequency.

In Fig. 6, the rotor displacements in one end of the shaft are shown while the rotor speed is zero. Similar behavior is observed in the other shaft end. Disregarding the electric noise, the error can be considered less than 0.03mm (7% of the airgap).

In Fig. 7, the rotor was rotating at 5600 rpm. In this case although oscillations happen, their amplitudes are less than 0.07mm (15% of the airgap).

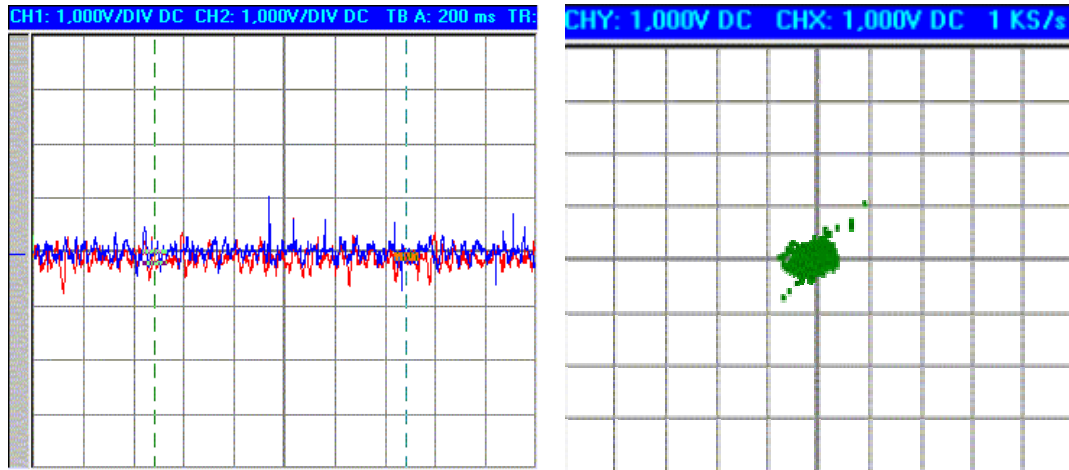


Fig. 6. Static response of two radial position controllers. Left: positions vs time, Right: horizontal vs vertical position. Scale: ver.:0.15mm/div, hor.:5ms/div.

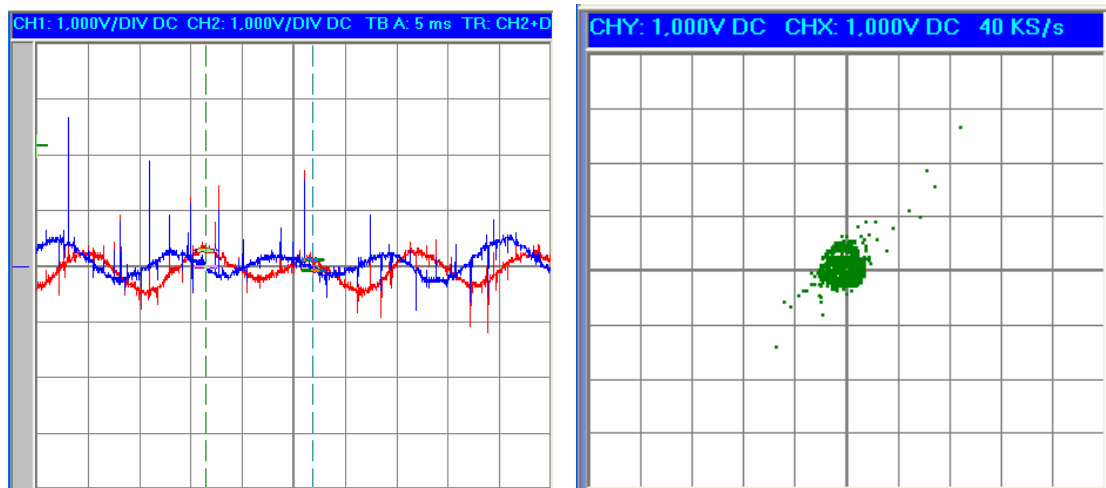


Fig. 7. Dynamic response of two radial position controllers while rotor speed is 5600 rpm. Left: positions vs time, Right: horizontal vs vertical position. Scale: ver.:0.15mm/div, hor.:5ms/div.

5. Conclusions

This work briefly has shown an industrial application of the so-called magnetic bearings.

The electromagnetic design of these devices was made in such a way to maintain the original external shape of the electric motor.

Modeling and design of the controlled system have been described and the digital implementation has been tested.

Experimental results, for a decentralized approach, were shown. They appear satisfactory.

6. Acknowledgements

The authors gratefully acknowledge the support of CNPq and CAPES.

7. References

ACESITA, www.acesita.com.br.

Åström, K.J. and Wittenmark, B., 1984, "Computer Controlled Systems", Prentice-Hall, Inc., Englewood Cliffs, N.J., USA, 430 p.

Chapetta, R.A., Santisteban, J.A., Noronha, R.F., 2002, "Mancais Magnéticos – Uma Metodologia de Projeto", Proceedings of the II Congresso Nacional de Engenharia Mecânica, CONEM 2002, João Pessoa, Brasil.

- Kyung, J.H. and Lee, C.W., 2002, "Controller Design for a Magnetically Suspended Milling Spindle Based on Chatter Stability Analysis", Proceedings of the Eighth International Symposium on Magnetic Bearings (ISMB-8), Mito, Japan, pp. 375-380.
- Noronha, R.F., Lima, L.T.G., Leite Jr., T.M., Gomes G.M.P. and Santos P.C.V., 2000, "Dynamic Behavior of a Magnetically Borne Rotor", Proceedings of the 16th International Conference on Magnetically Levitated Systems and Linear Drives – MAGLEV 2000, Rio de Janeiro, pp. 456-461.
- Ogata, K., 1970, "Engenharia de Controle Moderno", 4ª Ed., Prentice Hall do Brasil Ltda, 782 p.
- Ogata, K., 1994, "Discrete-Time Control Systems", Pearson Education.
- Santisteban, J.A., Mendes, S.R.A. and Sacramento D.S., 2003, "A Fuzzy Controller For An Axial Magnetic Bearing", Proceedings of the IEEE International Symposium on Industrial Electronics, Rio de Janeiro, Brazil, BD-000730.
- Santisteban, J.A., Noronha, R.F., David, D.F.B., Suhett, M.R. and Pedrosa, J.F.A., "Implementation of Magnetic Bearings on an Electric Motor", 2004, Proceedings of the VI Induscon, Joinville, SC, Brasil.
- Schweitzer, G., Bleuler, H. and Traxler, A., 1994, "Active Magnetic Bearings", v/dlf Hochschulverlag AG an der ETH Zürich, Suíça.

5. Responsibility notice

The authors are the only responsible for the printed material included in this paper.